A kinetic model of the central carbon metabolism for acrylic acid production in *Escherichia coli*

Alexandre Oliveira[1], Joana Rodrigues[1], Eugénio C. Ferreira[1], Lígia Rodrigues[1], Oscar Dias[1*]

[1] *Centre of Biological Engineering, University of Minho, Braga, Portugal*

* *Corresponding Author:* odias@deb.uminho.pt

ABSTRACT

Acrylic acid (AA) is a value-added chemical used in industry to produce diapers, coatings, paints, and adhesives, among many others. Due to its economic importance, there is currently a need for new and sustainable ways to synthesize it. Recently, the focus has been laid in the use of *Escherichia coli* to express the full bio-based pathway using 3-hydroxypropionate (3-HP) as an intermediary through three distinct pathways (Glycerol, malonyl-CoA, and β-alanine). Hence, the goals of this work were to assess which of the three pathways has a higher potential for industrial-scale production from either Glucose or Glycerol, and identify potential targets to improve the biosynthetic pathways yields.

The models developed during this work seem, when compared to the available literature, to successfully predict 3-HP production for the glycerol pathway, using Glycerol as carbon source, and for the malonyl-CoA and β-alanine pathways, using Glucose a carbon sources. Finally, this work allowed to identify four potential over-expression targets (G3pD, AccC, AspAT, and AspC) that should, theoretically, result in higher AA yields.

Keywords: Acrylic Acid, 3-Hydroxypropionate, *Escherichia coli*, Kinetic Model, *In silico* modelling, Systems Biology

Nomenclature

3-HPA - 3-hydroxypropionaldehyde	**3hpaD** - 3-hydroxypropionaldehyde dehydrogenase
3-HP - 3-hydroxypropionate	**3-HP-CoA** - 3-hydroxypropionyl-CoA
3hpcoaDH - 3-hydroxypropionyl-CoA dehydratase	**3hpcoaS** - 3-hydroxypropionyl-CoA synthase
AA - acrylic acid	**AA-CoA** - acrylyl-CoA
AccC - acetyl-CoA carboxylase	**AcoaTioE** - acrylyl-CoA thioesterase
AspAT - aspartate aminotransferase	**AspC** - aspartate carboxylase
BaAT - β-alanine aminotransferase	**CCM** - central carbon metabolism
DhaPT - dihydroxyacetone phosphate transferase	**FCC** - flux control coefficient
G3pD - glycerol-3-phosphate dehydrogenase	**G3pP** - glycerol-3-phosphate phosphatase
GluD - L-glutamate dehydrogenase	**Glu-Ba** – β-alanine route using Glucose as carbon source
Glu-Gly – Glycerol route using Glucose as carbon source	**Gly-Mcoa** – Malonyl-CoA route using Glucose as carbon source
GlyD - Glycerol dehydrogenase	**Gly-Ba** – β-alanine route using Glycerol as carbon source
GlyDH - Glycerol dehydratase	**Gly-Gly** – Glycerol route using Glycerol as carbon source
GlyK - glycerol kinase	**Gly-Mcoa** – Malonyl-CoA route using Glycerol as carbon source
MCA - metabolic control analysis	**McoaR** - malonyl-CoA reductase
MSA - malonic semialdehyde	**MsaR** - malonic semialdehyde reductase

1 – Introduction

Acrylic acid (AA) ($C_3H_4O_2$) is an important chemical compound that is one of the key components of superabsorbent polymers (Chu et al., 2015; Tong et al., 2016; Beerthuis et al., 2015). According to the Allied Market Research, in 2015, the global market for **AA** was valued at 12,500 million US dollars, and is expected to reach 19,500 million US dollars until 2022 (Allied Market Research, 2016). Despite its economic importance, the vast majority of **AA**

is still produced by the oxidation of propylene or propane in a purely chemical process (Chu et al., 2015; Beerthuis et al., 2015; Corma Canos et al.,2007; Unverricht et al., 2006). Ergo, the principal method for **AA** production was found to be expensive, with a high energy demand, thus contributing to the planet's environment decay. Hence, the development of an innovative and sustainable biological production method has been attracting the attention of the scientific community (Chu et al., 2015; Tong et al., 2016; Liu and Liu, 2016). In the last decade, several semi-biological methods have emerged and were optimized. These methods consist of the bio-based production of **3-hydroxypropionate (3-HP)** and its subsequent chemical conversion to **AA.** Despite the substantial improvements obtained with these methods, this process involves a catalytic step that increases the production costs and environmental impact due to high energy demands (Chu et al., 2015; Tong et al., 2016; Beerthuis et al., 2015; Corma Canos et al., 2007). Hence, the AA's production method should, ideally, be a bio-based direct route as, in theory, microbial feedstocks are less expensive, allowing a higher profit margin (Chu et al., 2015). Moreover, a more sustainable bioprocess allows to decrease non-renewable resources dependence and CO_2 emissions.

Fortunately, in recent years, it has been proven that it is possible to use engineered *Escherichia coli* to convert Glucose or Glycerol into **AA**. Like in the semi-biological methods, the bioprocess is also divided into two main parts, the production of **3-HP** and its subsequent conversion to **AA**. This part of the pathway, from **3-HP** to **AA,** has not been extensively studied. So far, there are only three studies that successfully converted Glucose or Glycerol to **AA** in *E.coli* (Chu et al., 2015; Tong et al., 2016; Liu and Liu, 2016). However, the synthesis of **3-HP** is well reported, and three distinct pathways have been identified, namely the glycerol route, the malonyl-CoA route, and the β-alanine route. From these pathways, it is well established that the glycerol pathway is associated with the highest yields. However, one of the reactions of this route requires the supplementation of vitamin B_{12} (Figure 1), which is an expensive practice at an industrial-scale production, hence a significant disadvantage of this route (Raj et al., 2008; Ashok et al., 2013).

The bio-based method is currently considered an up-and-coming alternative to the conventional process as the production of **3-HP** increased considerably in the last few years. Recently, studies reported productions of up to 8.10 g/L with the glycerol pathway (Chu et al., 2015), 3.60 g/L with the malonyl-CoA pathway (Liu et al., 2016), and 0.09 g/L with the β-alanine pathway (Song et al., 2016). However, the **AA** yields obtained by Tong et al. (2016) (0.0377 g/L) and Chu et al. (2015) (0.12 g/L) for the glycerol pathway, and Liu and Liu (2016) (0.013 g/L) for the malonyl-CoA pathway, established that this process still needs to be optimized to compete with the currently used methods.

Taking these considerations into account, the main goals of this work are to identify the reactions of the known routes for **AA** production (Glycerol, malonyl-CoA, and β-alanine pathways) and to determine which have a higher potential for industrial-scale production. The *E. coli's* **central carbon metabolism (CCM)** kinetic models will be used to analyze the three pathways using either Glucose or Glycerol as carbon source. Finally, novel optimization strategies to improve the **AA** yields of the three biosynthetic pathways will also be sought.

2 – Materials and Methods

2.1 – Kinetic Modelling

The dynamic model developed by Millard et al. (2017) was extended to include the missing pathways associated with **3-HP** and **AA** production. This process was divided into three steps, the extension of the **CCM** to include the production of the three intermediary compounds (Glycerol, malonyl-CoA, and β-alanine), the subsequent production of **3-HP**, and the production of **AA.**

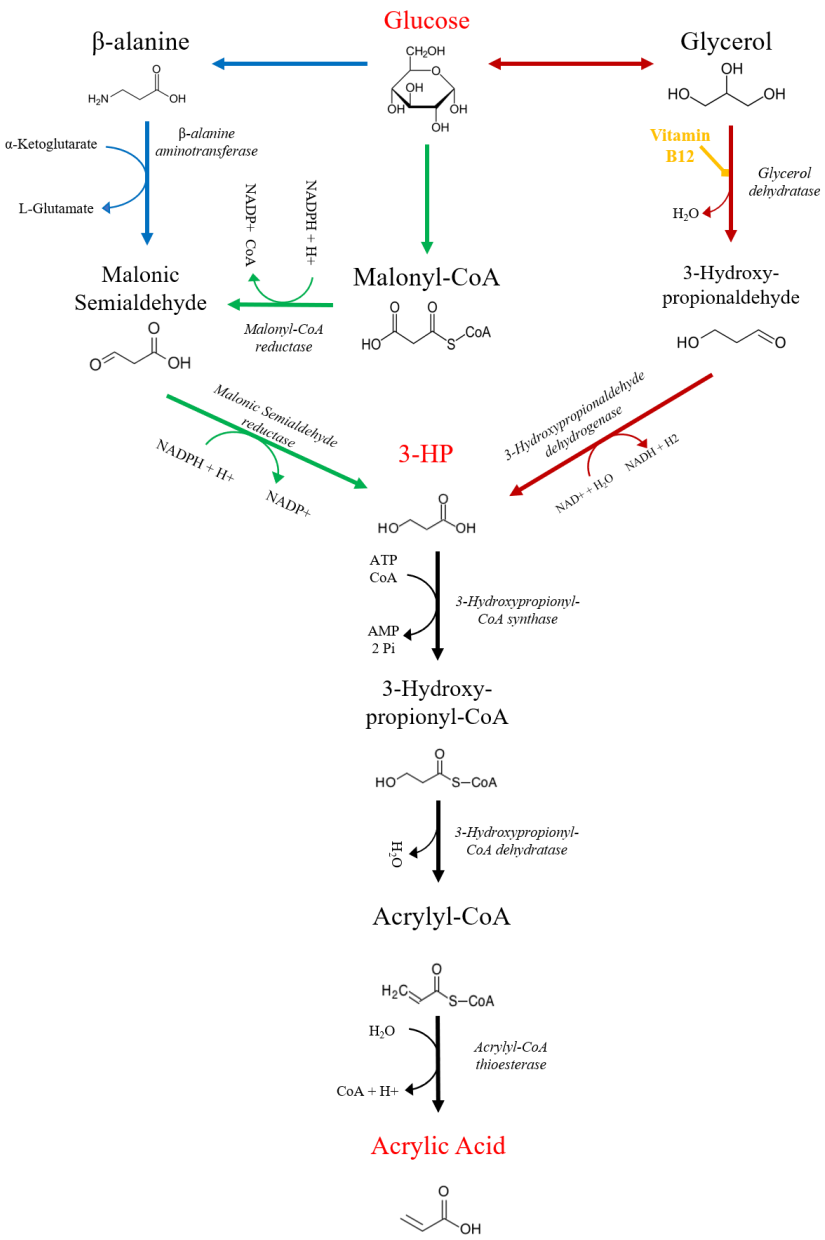

Figure 1. Biosynthetic pathways for the acrylic acid (AA) production in *Escherichia coli* from Glucose using 3-hydroxypropionate (3-HP) as an intermediary. 3-HP can be produced from Glucose through three distinct pathways: Glycerol (red arrows), malonyl-CoA (green arrows), and β-alanine (blue arrows). Furthermore, *E. coli* can also direct Glycerol towards the central carbon metabolism, allowing it to be used as a carbon source.

2.1.1 – Parameter Selection

Kinetic equations and their respective parameters were retrieved from the available literature. Databases like BioCyc (Caspi et al., 2018), BRENDA (Jeske et al., 2019), Sabio-RK (Wittig et al., 2018) and eQuilibrator (Flamholz et al., 2012) were used to identify the kinetic mechanism of each enzyme and obtain their respective parameters. Furthermore, instead of a single value, the average of all parameters found for each enzyme, excluding outliers, was used to obtain a better representation. A summary of the values considered when calculating the mean value for each reaction is presented in supplementary material A.

Regarding the parameters required to describe a reaction, the maximal rate (V_{max}) is usually not reported in the literature. Unfortunately, this parameter is highly dependent on the specificity of the assay conditions. Hence, the specific activity or the turnover (a.k.a. K_{cat}) are reported instead. Two distinct methods were used, as a workaround, to estimate values for this parameter. Method 1, adapted from the work of Chassagnole and colleagues (Chassagnole et al., 2002), was used for reactions belonging to *E. coli*'s native metabolism. Initially, a steady-state flux distribution is determined

for the original kinetic model. Then, a genome-scale model of *E. coli* K-12 MG1655 (in this case iML1515) (Monk et al., 2017) is used to predict the flux of the new reactions. For this purpose, the shared reactions between the kinetic model and the stoichiometric model are constrained to the previously determined flux distribution (±0.01 mM/s). Then, a flux variability analysis (Mahadevan and Schilling (2003)) is performed to estimate the maximum flux (*v*). By equalizing *v* to the respective rate law ($V_{max} \cdot \times F(X,K)$), the following equation is obtained:

$$v = V_{max} \cdot F(X,K) \Leftrightarrow V_{max} = \frac{v}{F(X,K)} \quad \textbf{(1)}$$

in which *X* is a vector of parameters, and *K* a vector of steady-state concentrations for the metabolites involved in the respective reaction. Furthermore, notice that for newly added metabolites, the steady-state concentration was assumed to be 1 mM. An example of these calculations and the resulting V_{max} values are presented in the supplementary material B, section 1.1.

Method 2 was used for reactions of the heterologous pathways. In this method, the V_{max} was estimated assuming that the total concentration of enzyme was in surplus (100 mM), thus calculating this parameter as shown in equation 2:

$$V_{max} = K_{cat} \cdot [E]_T \quad \textbf{(2)}$$

2.1.2 – Central Carbon Metabolism (CCM) Extension

The production of Glycerol, malonyl-CoA, and β-alanine had to be included in the model to insert the three heterologous pathways (Figure 2). The reactions catalyzed by the **glycerol-3-phosphate dehydrogenase (G3pD)** and **glycerol-3-phosphate phosphatase (G3pP)** are required to produce Glycerol from dihydroxyacetone phosphate. Considering that this route needs to be reversible to use Glycerol as a carbon source, reactions catalyzed by the **glycerol kinase (GlyK)**, **glycerol dehydrogenase (GlyD)** and the **dihydroxyacetone phosphate transferase (DhaPT)** were also included (Figure 2). As shown in Figure 2, only one reaction is required to obtain malonyl-CoA, namely the reaction catalyzed by the **acetyl-CoA carboxylase (AccC)**. Finally, three reactions were included for the β-alanine pathway. Two of these reactions are promoted by the **aspartate aminotransferase (AspAT)** and the **aspartate carboxylase (AspC)** enzymes, allowing the production of β-alanine, and one catalyzed by the **L-glutamate dehydrogenase (GluD**) enzyme to produce glutamate, which is required by the **AspAT** to produce aspartate (Figure 2) (Caspi et al., 2018; Kanehisa et al., 2018).

All reactions and their respective stoichiometry are shown below:

G3pD: Dihydroxyacetone phosphate + NADPH + H^+ = Glycerol-3-Phosphate + $NADP^+$ **(3)**

G3pP: Glycerol-3-Phosphate + H_2O → Glycerol + P_i **(4)**

GlyK: Glycerol + ATP → Glycerol-3-Phosphate + ADP + H^+ **(5)**

GlyD: Glycerol + NAD^+ → Dihydroxyacetone + NADH + H^+ **(6)**

DhaPT: Dihydroxyacetone + Phosphoenolpyruvate → Dihydroxyacetone phosphate + Pyruvate **(7)**

AccC: Acetyl-CoA + ATP + HCO_3 → Malonyl-CoA + ADP + P_i **(8)**

GluD: α-Ketoglutarate + NADPH + NH_4 = L-Glutamate + $NADP^+$ + H_2O **(9)**

AspAT: Oxaloacetate + L-Glutamate = L-Aspartate + α-Ketoglutarate **(10)**

AspC: Aspartate → β-alanine + CO_2 **(11)**

Furthermore, the kinetic law equation and the respective parameters for each of the previously described reactions are presented in table 1.

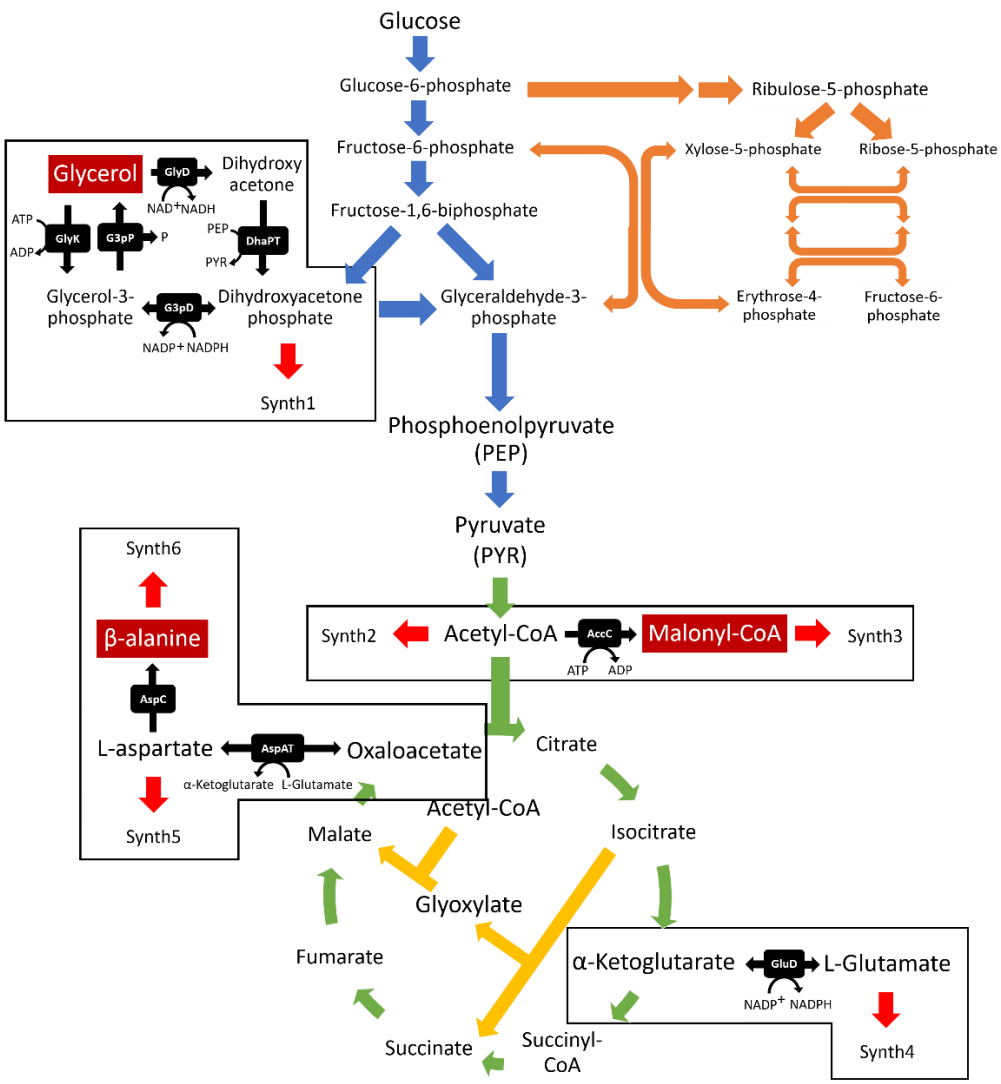

Figure 2. Representation of the central carbon metabolism of *Escherichia coli* and the reactions added to the kinetic model. The reactions depicted by the blue, orange, green and yellow arrows represent, respectively, the glycolysis, pentose-phosphate pathway, tricarboxylic acid cycle and the glyoxylate shunt, which are all present in the original model. The black arrows represent the nine reactions that were added to the model. More specifically, the glycerol-3-phosphate dehydrogenase (G3pD), the glycerol-3-phosphate phosphatase (G3pP), the glycerol kinase (GlyK), glycerol dehydrogenase (GlyD), and the dihydroxyacetone phosphate transferase (DhaPT) are required to obtain Glycerol. The acetyl-CoA carboxylase (AccC) is used to produce malonyl-CoA, and the aspartate aminotransferase (AspAT), the aspartate carboxylase (AspC) and the L-glutamate dehydrogenase (GluD) is required for β-alanine production. Finally, red arrows depict the Synth reactions added to account for the presence of the newly added metabolites in other pathways.

Furthermore, an additional set of pseudo-reactions were included in the model; the Synth reactions (Figure 2). These reactions were inspired by the work of Chassagnole et al. (2002) and Machado et al. (2014), and are used to represent the pathways involved in the breakdown of the newly added metabolites. For these reactions, mass action kinetics was assumed, and, using the same principle as Method 1, the sum of all fluxes from the reactions that metabolize each metabolite in the stoichiometric model was accounted to determine the *k* values for each synth reaction. The resulting *k* values are presented in the supplementary material B, section 1.2.

Table 1. Rate Law (RL) equations and parameters of the reactions that belong to the native metabolism of *E. coli*, and the respective references used to calculate the average value for each parameter. The following abbreviations were used: RERBB: Rapid Equilibrium Random Bi Bi; MM - Michaelis-Menten; RBB - Random Bi Bi; OBB - Order Bi Bi; PPBB - Ping-Pong Bi Bi; HC - Hill Cooperativity; MA - Mass Action.

Reaction	RL	Equation	Parameters	Reference
G3pD	RERBB	$V_{max} \cdot \frac{\left(\frac{A \cdot B - \left(\frac{P \cdot Q}{K_{eq}}\right)}{K_{m,a} \cdot K_{m,b}}\right)}{\left(1 + \frac{A}{K_{m,a}} \cdot \frac{B}{K_{m,b}}\right) + \left(1 + \frac{P}{K_{m,p}} \cdot \frac{Q}{K_{m,q}}\right) - 1}$	$K_{m,a}$ = 0.175 mM $K_{m,b}$ = 0.0037 mM $K_{m,p}$ = 0.12 mM $K_{m,q}$ = 0.165 mM K_{eq} = 900	Edgar and Bell (1978a) Edgar and Bell (1978b) Kito and Pizer (1969)
G3pP	MM	$V_{max} \cdot \frac{A}{K_m + A}$	K_m = 2.9 mM	Salles et al. (2007)
GlyK	RBB	$V_{max} \cdot \frac{A \cdot B}{K_{d,a} \cdot K_{m,b} + K_{m,b} \cdot A + K_{m,a} \cdot B + A \cdot B}$	$K_{m,a}$ = 0.0084 mM $K_{m,b}$ = 0.0049 mM $K_{d,a}$ = 0.086 mM	Pettigrew et al. (1990) Hayashi and Lin (1967) Thorner and Paulus (1973) Applebee et al. (2011)
AccC	OBB	$V_{max} \cdot \frac{A}{K_{m,A} \cdot \left(1 + \frac{P}{K_{i,P}}\right) + A} \cdot \frac{B}{K_{m,B} + B}$	$K_{m,a}$ = 0.018 mM $K_{m,b}$ = 0.06 mM $K_{i,p}$ = 0.07 mM	Soriano et al. (2005) Freiberg et al. (2004) Meades Jr et al. (2010)
GluD	MM	$V_{max} \cdot \frac{A}{K_{m,a} + A} \cdot \frac{B}{K_{m,b} + B}$	$K_{m,a}$ = 0.495 mM $K_{m,b}$ = 0.037 mM	Sharkey and Engel (2008) Sakamoto et al. (1975) Mantsälä and Zalkin (1976) Di Fraia et al. (2000)
AspAT	PPBB	$V_{max} \cdot \frac{\left(\frac{A \cdot B - \left(\frac{P \cdot Q}{K_{eq}}\right)}{K_{m,a} \cdot K_{m,b}}\right)}{\left(1 + \frac{A}{K_{m,a}} \cdot \frac{Q}{K_{m,q}}\right) \cdot \left(1 + \frac{B}{K_{m,b}} \cdot \frac{P}{K_{m,p}}\right)}$	$K_{m,a}$ = 19.07 mM $K_{m,b}$ = 0.19 mM $K_{m,p}$ = 0.437 mM $K_{m,q}$ = 2.94 mM K_{eq} =3.2	Yagi et al. (1985) Chow et al. (2004) Mavrides and Orr (1975) Deu et al. (2002) Fernandez et al. (2012)
AspC	MM	$V_{max} \cdot \frac{A}{K_m + A}$	K_m = 0.155 mM	Ramjee et al. (1997) Williamson and Brown (1979)
GlyD	HC	$V_{max} \cdot \frac{A^n}{(K_{m,a})^n + B^n} \cdot \frac{B^n}{(K_{m,b})^n + B^n}$	$K_{m,a}$ = 47.83 mM $K_{m,b}$ = 1.385 mM n =0.98	Piattoni et al. (2013) Zhang et al. (2010)
DhaPT	MA	$k \cdot A \cdot B$	Not Found	

2.1.3 – Pathways for Acrylic Acid Production

The following step was to insert the three heterologous pathways to produce **AA** separately into the extended **CCM** model. All the pathways are divided into two different phases, the production of an intermediary compound, namely **3-HP**, and subsequent production of **AA** (Figure 1).

The first phase involves two different enzymes in each pathway. Regarding the glycerol pathway, such enzymes are the **glycerol dehydratase (GlyDH)** and the **3-hydroxypropionaldehyde dehydrogenase (3hpaD)**. In the malonyl-CoA pathway, the **malonyl-CoA reductase (McoaR)** enzyme is responsible for the formation of **malonic semialdehyde (MSA),** which is then converted into **3-HP** by the **malonic semialdehyde reductase (MsaR)**. Finally, the β-alanine pathway also involves producing **MSA**, though by the **β-alanine aminotransferase (BaAT)** enzyme, and converting it to **3-HP** by the **MsaR**. The stoichiometry of these is shown below, and the respective kinetic parameters presented in Table 2.

GlyDH: Glycerol → 3-HPA + H_2O **(12)**

3hpaD: 3-HPA + NAD^+ + H_2O → 3-HPA + NADP + $2H^+$ **(13)**

McoaR: Malonyl-CoA + NADPH + H^+ → MSA + CoA + $NADP^+$ **(14)**

MsaR: MSA + NADPH + H^+ → 3-HP + $NADP^+$ **(15)**

BaAT: β-alanine + α-Ketoglutarate → MSA + L-Glutamate **(16)**

The final step is converting the newly formed **3-HP** into **AA**. This process involves the production of **3-hydroxypropionyl-CoA (3-HP-CoA)** by the **3-hydroxypropionyl-CoA synthase (3hpcoaS)**, the subsequent formation of **acrylyl-CoA (AA-CoA)** by the **3-hydroxypropionyl-CoA dehydratase (3hpcoaDH)**, and finally, the production of **AA** by the **acrylyl-CoA thioesterase (AcoaTioE)** enzyme, as shown in Figure 1. Likewise, the stoichiometry of these reactions is shown below, and the respective kinetic parameters presented in Table 2.

3hpcoaS: 3-HP + CoA + ATP → 3-HP-CoA + 2P + AMP **(17)**

3hpcoaDH: 3-HP-CoA → AA-CoA + H_2O **(18)**

AcoaTioE: AA-CoA + H_2O → AA + CoA + H^+ **(19)**

Table 2. Rate Law (RL) equations and parameters of the reactions of the three heterologous pathways (Glycerol, malonyl-CoA and β-alanine) required to produce acrylic acid and the respective references used to calculate the average value for each parameter

Reaction	RL	Equation	Parameters	Reference
GlyDH	Specific Activation	$\frac{E \cdot K_{cat} \cdot A \cdot Activator}{K_{m,a} \cdot K_a + (K_{m,a} + A) \cdot Activator}$	E = 100 mM K_{cat} = 0.0621 s^{-1} K_m = 6.15 mM K_a = 0.008 mM	Sauvageot et al. (2002) Schütz and Radler (1984)
3hpaD	Michaelis-Menten	$\frac{E \cdot K_{cat} \cdot A \cdot B}{K_{m,a} \cdot K_{m,b} + K_{m,b} \cdot A + K_{m,a} \cdot B + A \cdot B}$	E = 100 mM K_{cat} = 16.73 s^{-1} $K_{m,a}$ = 0.39 mM $K_{m,b}$ = 1.3 mM	Jo et al. (2008)
McoaR	Michaelis-Menten	$\frac{E \cdot K_{cat} \cdot A \cdot B}{K_{m,a} \cdot K_{m,b} + K_{m,b} \cdot A + K_{m,a} \cdot B + A \cdot B}$	E = 100 mM K_{cat} = 50 s^{-1} $K_{m,a}$ = 0.3 mM $K_{m,b}$ = 0.03 mM	Hügler et al. (2002) Liu et al. (2013)
MsaR	Michaelis-Menten	$\frac{E \cdot K_{cat} \cdot A \cdot B}{K_{m,a} \cdot K_{m,b} + K_{m,b} \cdot A + K_{m,a} \cdot B + A \cdot B}$	E = 100 mM K_{cat} = 115 s^{-1} $K_{m,a}$ = 0.07 mM $K_{m,b}$ = 0.07 mM	Kockelkorn and Fuchs (2009)
BaTA	Ping-Pong Bi Bi	$\frac{E \cdot K_{cat} \cdot A \cdot B}{K_{m,b} \cdot A + K_{m,a} \cdot B \cdot \left(1 + \frac{B}{K_{i,B}}\right) + A \cdot B}$	E = 100 mM K_{cat} = 47.4 s^{-1} $K_{m,a}$ = 5.8 mM $K_{m,b}$ = 1.07 mM $Ki_{,b}$ = 10.2 mM	Liu et al. (2005)
3hpcoaS	Michaelis-Menten	$E \cdot K_{cat} \cdot \frac{A}{K_{m,a} + A} \cdot \frac{B}{K_{m,b} + B} \cdot \frac{C}{K_{m,c} + C}$	E = 100 mM K_{cat} = 36 s^{-1} $K_{m,a}$ = 0.015 mM $K_{m,b}$ = 0.01 mM $K_{m,c}$ = 0.05 mM	Alber and Fuchs (2002)
3hpcoaDH	Michaelis-Menten	$\frac{E \cdot K_{cat} \cdot A}{K_m + A}$	E = 100 mM K_{cat} = 96 s^{-1} K_m = 0.06 mM	Teufel et al. (2009)
AcoaTioE	Michaelis-Menten	$\frac{E \cdot K_{cat} \cdot A}{K_m + A}$	E = 100 mM K_{cat} = 0.55 s^{-1} K_m = 0.167 mM	Zhuang et al. (2008)

Four models were created for each of the three pathways resulting in a total of twelve distinct models. To be more precise, for each pathway, models to produce **3-HP** or **AA**, from Glucose or Glycerol as carbon sources, were put forward. All models can be found at https://cutt.ly/aaKineticModels

2.2 – Time Course Simulation

Time course simulations were performed to assess **3-HP** and **AA** production over time. These simulations were conducted using a deterministic method (LSODA) from COPASI (Hoops et al., 2006), with a duration of three or six hours, to allow the consumption of all available carbon source. These simulations were conducted using Glucose and Glycerol as carbon sources. Since the available carbon sources have a different number of carbons, the initial concentration of such molecules had to ensure that the amount of carbon provided to the model was the same. Thus, the initial concentrations for Glucose and Glycerol were 55.5 mM (10 g/L) and 217.2 mM (20 g/L), respectively. Which allowed comparing both carbon sources, and the three pathways for each carbon source. Furthermore, the initial concentration of the carbon source was also set to replicate the initial conditions of published results, thus allowing to assess the model to available literature for these routes.

2.3 – Optimization Strategies

The first step was to determine the **flux control coefficient (FCC)**, through a **metabolic control analysis (MCA)**. Initially, a feed and drains for Glycerol, malonyl-CoA, β-alanine, and **AA** were included to replicate a continuous model and find a valid steady-state, which is required to determine the **FCCs.** Nevertheless, a batch version of the model was used for the optimization step. These coefficients reflect the control each reaction has over the formation of **AA**. The reaction with most influence was either over-expressed, under-expressed, or knocked-out through a change in the V_{max}, according to the respective coefficient. The new mutant strains were obtained using the automated optimization tool provided by COPASI (Hoops et al., 2006). The goal of the optimization was not to meticulously predict the final concentration of **AA**, but rather to find promising targets for optimization. Hence, the changes in the V_{max} were limited to 50 times the original value to allow overcoming the *in silico* influence of such reaction, while not impairing the *in vivo* implementation.

The objective function was the maximization of **AA** concentration in the time course task. After creating new mutants, this process was repeated to further optimize the mutant strains. The task eventually stopped when either the glucose feed was limiting the production of **AA**, the limiting reaction was already optimized, or the system could no longer reach a stable steady-state point during the **MCA**.

3 – Results and Discussion

3.1 – Time Course Simulation

Regarding the glycerol pathway using Glucose (**Glu-Gly**) and Glycerol (**Gly-Gly**) as carbon source, the **3-HP** models' simulations predicted, respectively, the production of 0.19 g/L after three hours, and 8.30 g/L after six-hours (Figure 3). Whereas, concerning the production of **AA**, the **Glu-Gly** and **Gly-Gly** models predicted 0.16 g/L and 6.71 g/L, respectively (Figure 4). From these results, it seems that Glycerol is associated with higher yields, which is in good agreement with what is reported in the available literature (Chu et al., 2015). Moreover, regarding the production of **AA**, the intracellular concentration of **3-HP** showed that there is no accumulation (Figure 4), meaning that the most **3-HP** is converted into **AA**. These results are most likely associated with the use of excessive enzyme concentration to calculate the V_{max} for the heterologous pathway, which led to a situation where the main limiting factor in the synthesis of **AA** was the **CCM's** fluxes distribution. However, this is not the case *in vivo*, as the works that tested the full bio-based route show that **3-HP** and other intermediates indeed accumulate during this process (Chu et al., 2015; Tong et al., 2016).

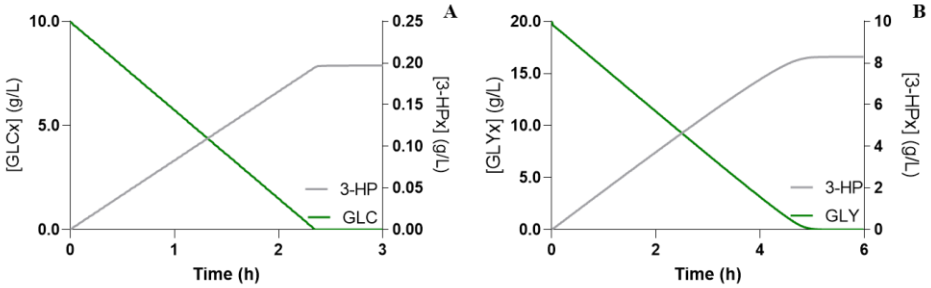

Figure 3. Simulation results for 3-hydroxypropionate (3-HP) production via the glycerol pathway. A - Glucose (GLCx) consumption and variation of extracellular 3-HP (3-HPx) over time; B - Glycerol (GLYx) consumption and variation of 3-HPx over time.

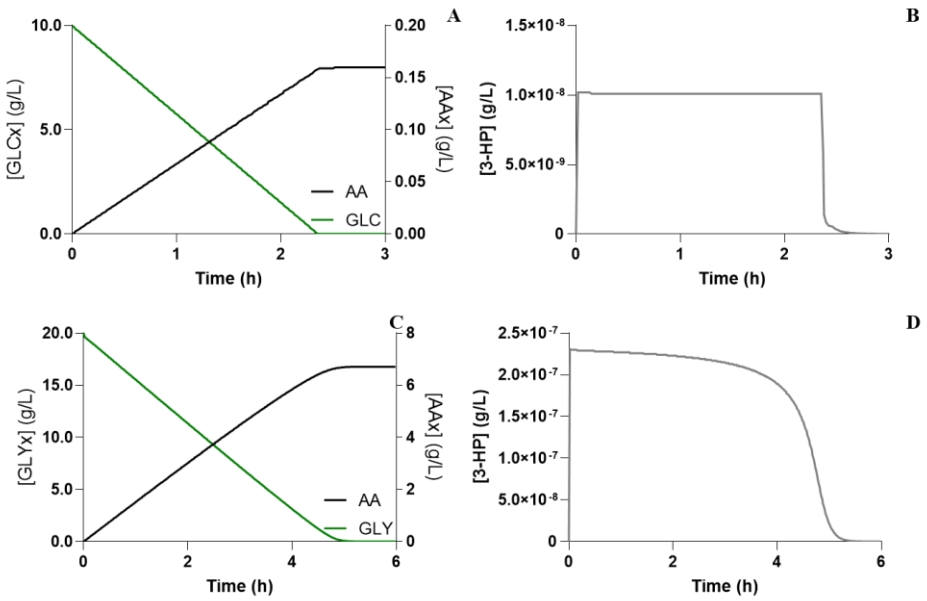

Figure 4. Simulation results for acrylic acid (AA) production via the glycerol pathway. A - Glucose (GLC) consumption and variation of extracellular AA (AAx) over time; B – Variation of 3-hydroxypropionate (3-HP) concentration over time when using Glucose as carbon source; C - Glycerol (GLYx) consumption and variation of extracellular AAx over time; D - Variation of 3-HP concentration over time when using Glycerol as carbon source.

When comparing the predicting capabilities of glycerol pathway models (Table 3), it is possible to observe that the predicted **3-HP** concentration, with the **Gly-Gly** model, is slightly different from what has been reported in the literature. This difference somewhat increases when increasing the initial concentration of carbon. For instance, for 40 g/L of Glycerol, the predicted production is about two times higher. Nevertheless, the model representing the **3-HP** production from Glycerol exhibits promising results.

The scenario with the **Glu-Gly** model is rather distinct, as it predicted a ten-fold lower concentration of **3-HP**. This difference might be associated with the production of Glycerol, more specifically, in the flux through **G3pD** and **G3pP,** as according to Chu et al. (2015) their strain is able to accumulate more Glycerol (2.5 g/L) than this model is able to produce (0.34 g/L), for the same amount of Glucose. Unfortunately, the study by Chu et al. (2015), which presented the highest **AA** concentration (0.12 g/L) reported thus far, did not disclose the amount of Glucose used to obtain such production; hence, it was not possible to directly compare the predicted titer from the **Gly-Gly** model. However, when performing simulation using glucose concentrations of 10 g/L and 20 g/L, the model predicts the production of 0.16 g/L and 0.32 g/L of **AA**, respectively. These results show that the **AA** production predicted by our model would be in good agreement with the results reported by Chu *et al.* (2015), if 10 g/L of Glucose had been used for the carbon source.

However, the model does not accumulate any intermediary compounds of the heterologous pathway; thus, most **3-HP** is converted into **AA**, which does not correctly represent the *in vivo* results. Therefore, when assessing the results of Tong et al. (2016), as expected, the model fails to predict the AA yield accurately.

Table 3. Literature review on 3-hydroxypropionate (3-HP) and acrylic acid (AA) production yields by the glycerol pathway in metabolically engineered *Escherichia coli*, and comparison with the yields predicted by the dynamic models using the same initial carbon concentration.

Reference	End Product	Carbon Source	Initial Carbon Conc. (g/L)	Titer (g/L)	Predicted Titer (g/L)
Raj et al. (2009)	3-HP	Glycerol	9.20	2.80	3.59
Rathnasingh et al. (2009)	3-HP	Glycerol	18.40	4.40	7.59
Chu et al. (2014)	3-HP	Glycerol	40.00	7.40	17.19
Chu et al. (2015)	3-HP	Glycerol	40.00	8.10	17.19
		Glucose	21.50	3.90	0.42
Tong et al. (2016)	AA	Glycerol	20.00	0.037	8.30

Regarding the malonyl-CoA pathway, a titer of 1.99 g/L, using Glucose (**Glu-Mcoa**), and 1.99 g/L, using Glycerol (**Gly-Mcoa**), of **3-HP** was predicted (Figure 5). Moreover, the **Glu-Mcoa** and **Gly-Mcoa** models also predicted 1.62 g/L and 0.17 g/L of **AA**, respectively (Figure 6). The analysis of the behavior of the model shows a considerable intracellular accumulation of dihydroxyacetone in the **Gly-Mcoa** model (Figure 5 - C). Hence, most carbon provided does not reach the **CCM**, and therefore these results should not be considered as it is not possible to conclude which is the best carbon source to produce **AA**. Despite that, literature reports suggest a consensus towards the use of Glucose as carbon source. However, it should be mentioned that no work using Glycerol was found. Thus, Glycerol cannot be excluded as a promising alternative carbon source.

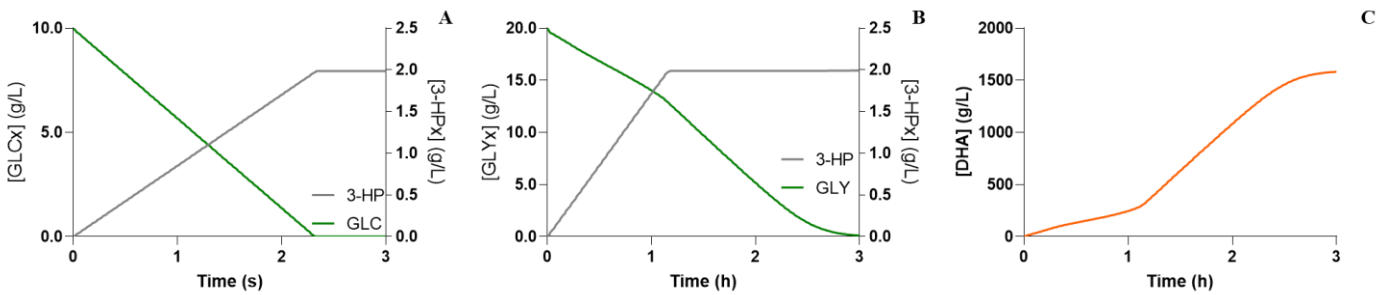

Figure 5. Simulation results for 3-hydroxypropionate (3-HP) production via the malonyl-CoA pathway. A - Glucose (GLCx) consumption and variation of extracellular 3-HP (3-HPx) over time; B - Glycerol (GLYx) consumption and variation of 3-HPx over time; C - Variation of intracellular dihydroxyacetone (DHA) concentration over time when using Glycerol.

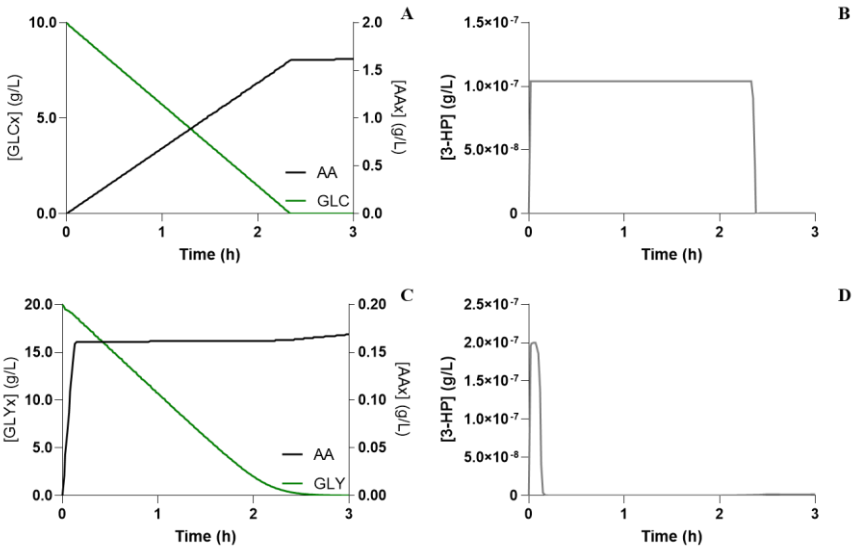

Figure 6. Simulation results for acrylic acid (AA) production via the malonyl-CoA pathway. A - Glucose (GLC) consumption and variation of extracellular AA (AAx) over time; B – Variation of 3-hydroxypropionate (3-HP) concentration over time when using Glucose as carbon source; C - Glycerol (GLYx) consumption and variation of extracellular AAx over time; D - Variation of 3-HP concentration over time when using Glycerol as carbon source.

Regarding the predicting capabilities of the **Glu-Mcoa** models, the predicted values are very similar to those found in the literature concerning **3-HP** production (Table 4), revealing an accurate prediction. However, the models failed to predict the production of **AA** since, as in the glycerol pathway, Liu and Liu (2016) reported the accumulation of **3-HP**, which was not replicated by the model (Figure 6).

Table 4. Literature review on 3-hydroxypropionate (3-HP) and acrylic acid (AA) production yields by the malonyl-CoA pathway in metabolically engineered *Escherichia coli*, and comparison with the yields predicted by the dynamic models using the same initial carbon concentration.

Reference	End Product	Carbon Source	Initial Carbon Conc. (g/L)	Titer (g/L)	Predicted Titer (g/L)
Cheng et al. (2016)	3-HP	Glucose	10.00	1.80	1.99
Liu et al. (2016)	3-HP	Glucose	20.00	3.60	3.96
Liu and Liu (2016)	AA	Glucose	20.00	0.013	3.22

Finally, regarding the β-alanine pathway, the models predicted a production of 0.034 g/L of **3-HP** and 0.041 g/L of **AA** using Glycerol (**Gly-Ba**), and 0.033 g/L of **3-HP** and 0.027 g/L of **AA** using glucose (**Gly-Ba**) (Figure 7 and 8). Again, the models did not predict the accumulation of **3-HP** that, although desirable, does not reflect the reality. Furthermore, regarding carbon sources, results point to a slight advantage towards Glycerol, even though, when compared to previous pathways, both produced a considerably lower concentration of **AA**. However, there seems to be a consensus towards using Glucose as carbon source, as to the best of our knowledge, no studies using the glycerol pathway have been reported.

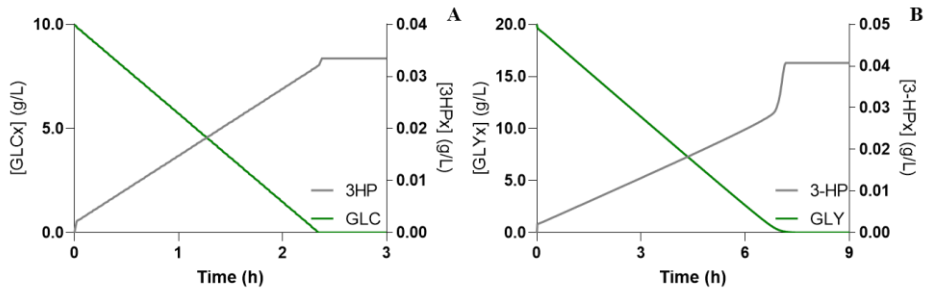

Figure 7. Simulation results for 3-hydroxypropionate (3-HP) production via the β-alanine pathway. A - Glucose (GLCx) consumption and variation of extracellular 3-HP (3-HPx) over time; B - Glycerol (GLYx) consumption and variation of 3-HPx over time.

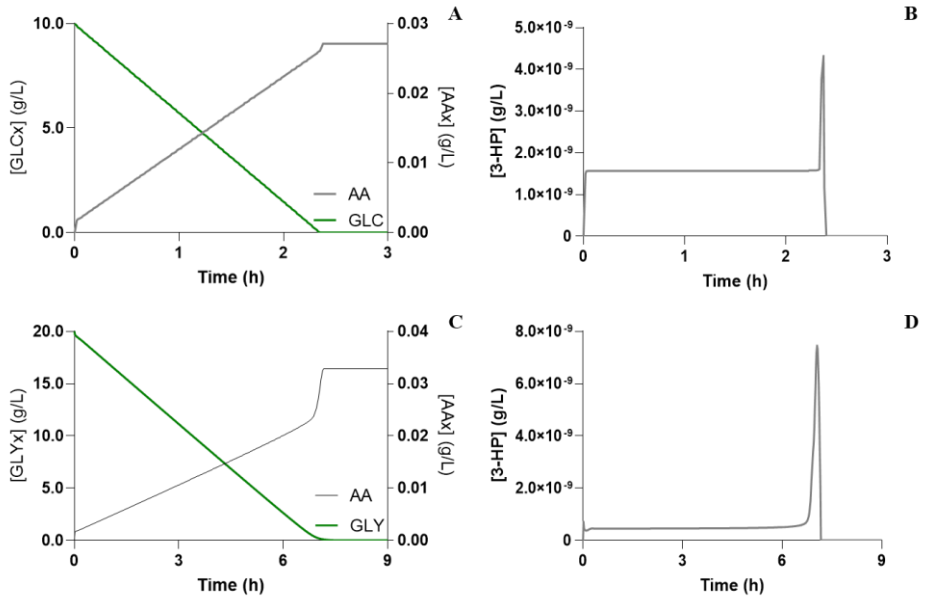

Figure 8. Simulation results for acrylic acid (AA) production via the β-alanine pathway. A - Glucose (GLC) consumption and variation of extracellular AA (AAx) over time; B – Variation of 3-hydroxypropionate (3-HP) concentration over time when using Glucose as carbon source; C - Glycerol (GLYx) consumption and variation of extracellular AAx over time; D - Variation of 3-HP concentration over time when using Glycerol as carbon source.

Moreover, the β-alanine pathway is the least studied, with very few reports, which might be associated with the fact that such studies reported significantly lower yields, when compared with the previous pathways (Liu et al., 2017). In fact, the authors only found one study concerning **3-HP** synthesis in *E. coli* using batch cultures (Song et al., 2016), while works in which **AA** is produced through this route are yet to be published. Despite that, the β-alanine model showed a promising predicting capability, at least when comparing to the results published by Song et al. (2016) (Table 5).

Table 5. Literature review on 3-hydroxypropionate (3-HP) and acrylic acid (AA) production yields by the β-alanine pathway in metabolically engineered *Escherichia coli*, and comparison with the yields predicted by the dynamic models using the same initial carbon concentration.

Reference	End Product	Carbon Source	Initial Carbon Conc. (g/L)	Titer (g/L)	Predicted Titer (g/L)
Song et al. (2016)	3-HP	Glucose	15.00	0.09	0.049

3.2 – Optimization Strategies

Ideally, the search for optimization targets should be performed in all six **AA** producing models. However, as mentioned before, the **Gly-Mcoa** model presented issues with dihydroxyacetone accumulation, not being further used in this work. Moreover, the **Gly-Gly** and **Gly-Ba** models, presented several instabilities when performing the **MCA**, not allowing to determine the **FCC** due to the lack of a steady-state. Henceforth, only the models designed to use Glucose as carbon source (**Glu-Gly, Glu-Mcoa, Glu-Ba**) were optimized.

Starting with the glycerol model, the **MCA** showed that the enzyme with the highest **FCC**, and thus a greater influence on **AA** production, was the **G3pD** (Figure 9), which is responsible for converting dihydroxyacetone phosphate into glycerol-3-phosphate. The reaction catalyzed by this enzyme is a potential bottleneck in the pathway, thus a target for overexpression. Using COPASI's optimization task, Mutant 1 was created, in which the best V_{max} of the selected reaction was 1.392 mM/s, representing a nearly 45-fold increase that resulted in the production of 3.11 g/L of **AA** (Figure 10). A subsequent **MCA** was performed using Mutant 1, aiming at further optimization of the obtained yields. However, after the previous iteration, the model could not reach a stable steady-state. Hence, the **FCCs** were not available, thus terminating the optimization of this pathway.

In the malonyl-CoA pathway, the **FCCs** allowed the identification of one possible overexpression target, the **AccC** (Figure 9), which is responsible for the conversion of acetyl-CoA to malonyl-CoA. It was then determined that the optimum V_{max} for this enzyme was 0.568 mM/s, corresponding to approximately a 2-fold overexpression. Mutant 1 was then created, producing a 3.11 g/L of **AA**, which corresponds to a 1.5 times higher yield than Mutant 0 (Figure 10). Unfortunately, a second iteration revealed that, once again, the model was unable to reach a steady-state. Thus, it was not possible to identify other potential targets using this methodology.

Regarding the β-alanine pathway, the **MCA** showed that the model has several reactions affecting the **AA** yield, but the reaction with the most significant impact is catalyzed by the enzymes encoded by gene **AspAT** (Figure 9). This reaction is responsible for aspartate production from oxaloacetate and L-glutamate, in turn, converted to β-alanine. This reaction has a positive coefficient, which indicates that it is a potential bottleneck impairing the downstream flux towards the heterologous pathway; thus, the optimization goal was to overexpress this enzyme. COPASI estimated that a 50-fold overexpression, resulting in a V_{max} of 127.4869 mM/s, was ideal for maximizing the production yields. With this change, the predicted **AA** concentration was 0.97 g/L, which corresponds to a 28-fold increase (Figure 10). A subsequent **MCA** revealed that the main limiting factor to **AA** production in Mutant 1 was the amount of Glucose provided to the model; hence the optimization was terminated with only one target identified. Similarly, the **AspC** gene, which is responsible for the production of β-alanine, can also be considered as a limiting factor for pathway flux, thus becoming a target for optimization, as the V_{max} was increased for the β-alanine model to work correctly (supplementary material B, section 1.1).

The goal of these optimizations was to provide guidelines that can be later implemented *in vivo* and not predict the AA production accurately. Nonetheless, the final concentrations that were obtained with the new mutants were used to compare with previous results. As shown in Table 6, the same concentration of **AA** (3.11 g/Ls) was produced by the glycerol and malonyl-CoA pathways. The β-alanine pathway also showed a large yield increase (0.97 g/L). However, the value is still considerably lower than the obtained with remaining pathways.

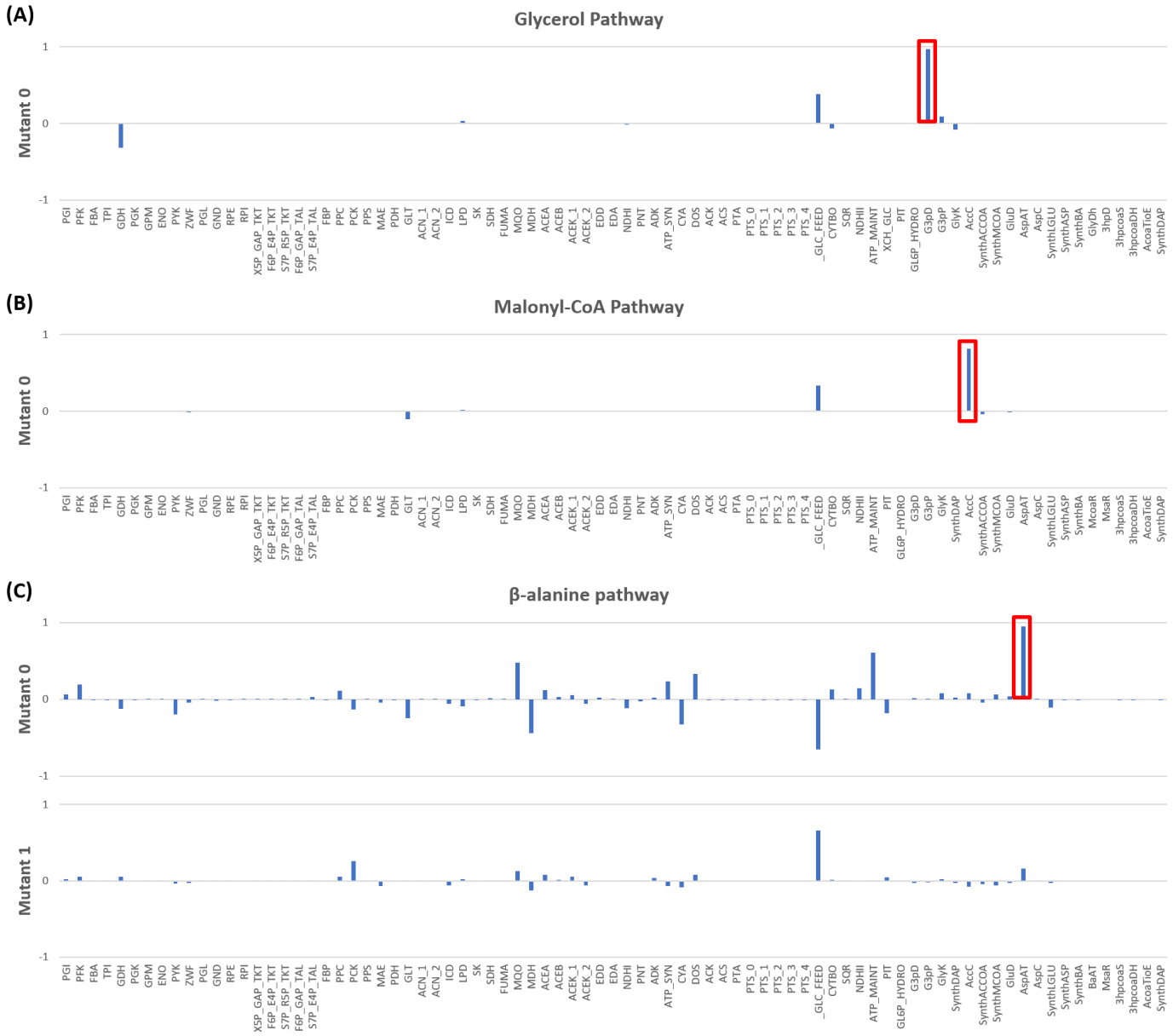

Figure 9. Flux Control Coefficients (FCC) results for acrylic acid formation, where the reaction with the most impact in the yield is highlighted in red. A – Results for the glycerol pathway. According to the coefficients the reaction with the most impact is the glycerol-3-phosphate dehydrogenase (G3pD), which due to its positive FCC is a potential target for overexpression; B – Results for the malonyl-CoA pathway. The results showed that the acetyl-CoA carboxylase (AccC) is a potential bottleneck in the pathway due to the positive FCC, hence another target for overexpression; C – Results for the β-alanine pathway. The highest FCC was for the aspartate aminotransferase (AspAT) which appears to be an ideal target for an overexpression.

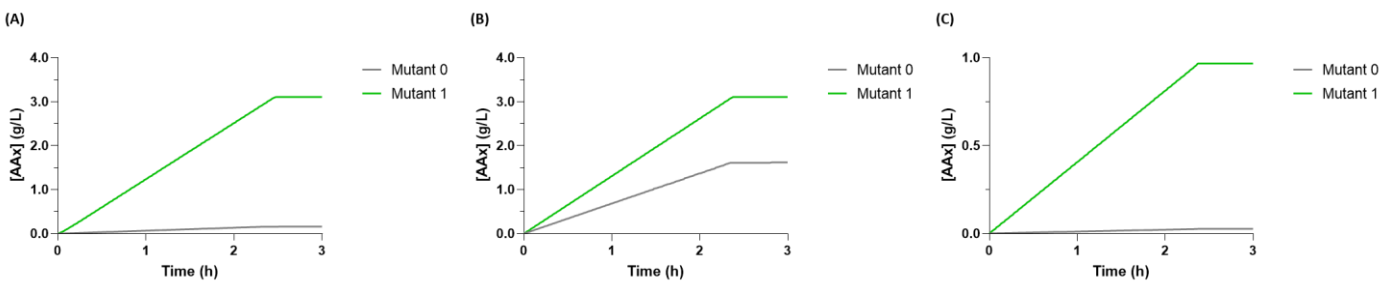

Figure 10. Comparison between the original acrylic acid (AA) production with the results obtained for the mutants developed with the optimization strategies identified. A – AA production of the glycerol pathway. Mutant 0 represents the model with the heterologous pathway, and Mutant 1 the same model with a 45-fold increase in the V_{max} of the G3pD reaction; B – AA production for the malonyl-CoA pathway. Mutant 0 represents the model with the heterologous pathway, and Mutant 1 the same model with a 2.5-fold increase in the V_{max} of the AccC; C – AA production for the β-alanine pathway. Mutant 0 represents the model with the heterologous pathway, and Mutant 1 the same model with a 50-fold increase in the Vmax of the AspAT.

Table 6. Summarized results of acrylic acid production for the mutant strains developed for the Glycerol, malonyl-CoA, and β-alanine models, using 10g/L of Glucose as substrate.

Pathway	Strain	Titer (g/L)
Glycerol	Mutant 0	0.16
	Mutant 1	3.11
Malonyl-CoA	Mutant 0	1.62
	Mutant 1	3.11
β-alanine	Mutant 0	0.027
	Mutant 1	0.97

4 – Conclusion

This present work resulted in twelve distinct models that allow predicting **3-HP** and **AA** production using either Glucose or Glycerol as carbon sources. When comparing the *in silico* results with published *in vivo* results, the models seem to be more accurate in predicting **3-HP** synthesis. The enzyme concentration used to determine the V_{max} for the heterologous enzymes was set not to limit the reaction flux, which is obviously not the case *in vivo*. An effort was put forward towards finding proteomics data that included the absolute quantification of such enzymes to circumvent this limitation. However, to the best of our knowledge, no quantification data has been reported for the selected enzymes; therefore, it will be important in the future to seek such data or, in the lack of new data, to determine it experimentally. In addition, issues were found in the **Glu-Gly**, **Gly-Mcoa**, and **Gly-Ba** models. These issues seem to be associated with the enzymes responsible for the production or assimilation of Glycerol. Thus, it is important to experimentally determine the kinetic parameters for these reactions to obtain better predictions. Another enzyme that hindered the analysis was the **AspC**, as the V_{max} determined initially using Method 1 was constraining the production of β-alanine. Hence, the V_{max} was recalculated using Method 2 (supplementary material B, section 1.1). Likewise, the experimental characterization of the kinetic parameters of this enzyme seems to be relevant to further improve these models.

An overall best carbon source does not emerge from the analysis of the models developed in this work. Instead, the answer is specific to each pathway. When the goal is to implement the glycerol pathway, it may be advantageous to use Glycerol since, as supported by the literature (Chu et al., 2015), it follows a straight path towards **AA** biosynthesis. For the malonyl-CoA pathway, results were not sufficiently robust to suggest that a carbon source would provide better yields, as the Gly-Mcoa model did not accurately predict the reported data. Glucose was the only carbon source reported in the literature, suggesting that it should be more advantageous, although it cannot be confirmed without a direct comparison. Finally, for the β-alanine pathway, the results pointed to a slight advantage of using Glycerol as carbon source; however, in the lack of published data, this cannot be confirmed.

This work allowed comparing the three bio-based routes for **AA** production. The results of these models suggest that the glycerol pathway leads to the highest yields, when combined with the use of Glycerol as the carbon source. Although this pathway is well established (Liu and Liu, 2016), a relevant caveat must be recalled. This pathway involves a reaction that relies on the presence of vitamin B_{12}, which represents a significant economic disadvantage at an industrial-scale production (Raj et al., 2008; Ashok et al., 2013). Hence, to make this route economically viable, either the yield must be significantly improved to overcome the cost of the vitamin supplementation, or a cheaper way to produce B_{12} must be found. Therefore, despite producing less **AA**, it seems to be beneficial to use the malonyl-CoA route, since it led to the second higher yield, does not need any vitamin supplementation, and there is still room for optimization (Borodina et al., 2015; Liu et al., 2017; Cheng et al., 2016).

The purpose of the suggested overexpression targets seems to be to direct more flux towards the formation of either Glycerol, malonyl-CoA, or β-alanine, thus increasing their bioavailability for the respective heterologous pathway. In total, four targets are suggested, the **G3pD** for the glycerol pathway, the **AccC** for the malonyl-CoA pathway, and the **AspAT** and **AspC** for the β-alanine pathway. A final aspect to consider for the optimization of the **AA** yields is that this model only comprises the **CCM**. Hence, other pathways that are not accounted for in the model are certainly diverting flux from **AA** synthesis. Hence, other strategies and targets may prove to be effective in forcing more flux towards the heterologous pathway, thus increasing the pathway yields.

Finally, after the improvement of the model, the final step should be the validation of the results with *in vivo* experiments. Therefore, the three heterologous routes should be implemented using both carbon sources, and the optimization strategies tested, to further confirm the *in silico* results herein gathered.

References

Alber, B. and Fuchs, G. (2002). Propionyl-coenzyme a synthase from Chloroflexus aurantiacus, a key enzyme of the 3-hydroxypropionate cycle for autotrophic CO2 fixation. Journal of Biological Chemistry, 277(14):12137–12143.

Applebee, M., Joyce, A., Conrad, T., Pettigrew, D., and Palsson, B. (2011). Functional and metabolic effects of adaptive glycerol kinase (GLPK) mutants in Escherichia coli. Journal of Biological Chemistry, 286(26):23150–23159.

Ashok, S., Sankaranarayanan, M., Ko, Y., Jae, K., Ainala, S., Kumar, V., and Park, S. (2013). Production of 3-hydroxypropionic acid from Glycerol by recombinant Klebsiella pneumoniae ΔdhaTΔyqhD which can produce vitamin B12 naturally. Biotechnology and Bioengineering, 110(2):511–524.

Beerthuis, R., Rothenberg, G., and Shiju, N. (2015). Catalytic routes towards acrylic acid, adipic acid and ϵ-caprolactam starting from biorenewables. Green Chemistry, 17(1):1341–1361.

Borodina, I., Kildegaard, K., Jensen, N., Blicher, T., Maury, J., Sherstyk, S., Schneider, K., Lamosa, P., Herrgård, M., Rosenstand, I., Öberg, F., Forster, J., and Nielsen, J. (2015). Establishing a synthetic pathway for high-level production of 3-hydroxypropionic acid in Saccharomyces cerevisiae via β-alanine. Metabolic Engineering, 27(1):57–64.

Caspi, R., Billington, R., Fulcher, C., Keseler, I., Kothari, A., Krummenacker, M., Latendresse, M., Midford, P., Ong, Q., Ong, W., Paley, S., Subhraveti, P., and Karp, P. (2018). The MetaCyc database of metabolic pathways and enzymes. Nucleic Acids Research, 46(1):633–639.

Chassagnole, C., Noisommit-Rizzi, N., Schmid, J., Mauch, K., and Reuss, M. (2002). Dynamic modeling of the central carbon metabolism of Escherichia coli. Biotechnology and Bioengineering, 79(1):53–73.

Cheng, Z., Jiang, J., Wu, H., Li, Z., and Ye, Q. (2016). Enhanced production of 3-hydroxypropionic acid from Glucose via malonyl-CoA pathway by engineered Escherichia coli. Bioresource technology, 200(1):897–904.

Chow, M., McElroy, K., Corbett, K., Berger, J., and Kirsch, J. (2004). Narrowing substrate specificity in a directly evolved enzyme: the A293D mutant of aspartate aminotransferase. Biochemistry, 43(40):12780–12787.

Chu, H., Ahn, J., Yun, J., Choi, I., Nam, T., and Cho, K. (2015a). Direct fermentation route for the production of acrylic acid. Metabolic Engineering, 32(1):23–29.268

Chu, H., Kim, Y., Lee, C., Lee, J., Jung, W., Ahn, J., Song, S., Choi, I., and Cho, K. (2015b). Metabolic engineering of 3-hydroxypropionic acid biosynthesis in Escherichia coli. Biotechnology and bioengineering, 112(2):356–364.

Corma Canos, A., Iborra, S., and Velty, A. (2007). Chemical routes for the transformation of biomass into chemicals. Chemical Reviews, 107(1):2411–2502.

Deu, E., Koch, K., and Kirsch, J. (2002). The role of the conserved Lys68*: Glu265 intersubunit salt bridge in aspartate aminotransferase kinetics: multiple forced covariant amino acid substitutions in natural variants. Protein Science, 11(5):1062–1073.

Di Fraia, R., Wilquet, V., Ciardiello, M. A., Carratore, V., Antignani, A., Camardella, L., Glansdorff, N., and di Prisco, G. (2000). Nadp+-dependent glutamate dehydrogenase in the antarctic psychrotolerant bacterium Psychrobacter sp. tad1: Characterization, protein and dna sequence, and relationship to other glutamate dehydrogenases. European journal of biochemistry, 267(1):121–131.

Edgar, J. and Bell, R. (1978a). Biosynthesis in Escherichia coli of m-glycerol 3-phosphate, a precursor of phospholipid. In vitro, 3(5):6.

Edgar, J. and Bell, R. (1978b). Biosynthesis in Escherichia coli of sn-glycerol 3-phosphate, a precursor of phospholipid. Kinetic characterization of wild type and feedback-resistant forms of the biosynthetic sn-glycerol-3-phosphate dehydrogenase. Journal of Biological Chemistry, 253(18):6354–6363.

Fernandez, F., de Vries, D., Penã-Soler, E., Coll, M., Christen, P., Gehring, H., and Vega, M. (2012). Structure and mechanism of a cysteine sulfinate desulfinase engineered on the aspartate aminotransferase scaffold. Biochimica et Biophysica Acta (BBA)-Proteins and Proteomics, 1824(2):339–349.

Flamholz, A., Noor, E., Bar-Even, A., and Milo, R. (2012). eQuilibrator—the biochemical thermodynamics calculator. Nucleic Acids Research, 40(1):D770–D775.

Freiberg, C., Brunner, N., Schiffer, G., Lampe, T., Pohlmann, J., Brands, M., Raabe, M., Häbich, D., and Ziegelbauer, K. (2004). Identification and characterization of the first class of potent bacterial acetyl-CoA carboxylase inhibitors with antibacterial activity. Journal of Biological Chemistry, 279(25):26066–26073.

Hayashi, S. and Lin, E. (1967). Purification and properties of glycerol kinase from Escherichia coli. Journal of Biological Chemistry, 242(5):1030–1035.

Hoops, S., Gauges, R., Lee, C., Pahle, J., Simus, N., Singhal, M., Xu, L., Mendes, P., and Kummer, U. (2006). COPASI - a complex pathway simulator. Bioinformatics, 22(24):3067–3074.

Hügler, M., Menendez, C., Schägger, H., and Fuchs, G. (2002). Malonyl-coenzyme a reductase from Chloroflexus aurantiacus, a key enzyme of the 3-hydroxypropionate cycle for autotrophic CO2 fixation. Journal of Bacteriology, 184(9):2404–2410.

Jeske, L., Placzek, S., Schomburg, I., Chang, A., and Schomburg, D. (2019). Brenda in 2019: a european elixir core data resource. Nucleic Acids Research, 47(1):542–549.

Jo, J., Raj, S., Rathnasingh, C., Selvakumar, E., Jung, W., and Park, S. (2008). Cloning, expression, and characterization of an aldehyde dehydrogenase from Escherichia coli K-12 that utilizes 3-hydroxypropionaldehyde as a substrate. Applied Microbiology and Biotechnology, 81(1):51.

Kanehisa, M., Sato, Y., Furumichi, M., Morishima, K., and Tanabe, M. (2018). New approach for understanding genome variations in KEGG. Nucleic Acids Research, 47(1):590–595.

Kito, M. and Pizer, L. (1969). Purification and regulatory properties of the biosynthetic L-glycerol 3-phosphate dehydrogenase from Escherichia coli. Journal of Biological Chemistry, 244(12):3316–3323.

Kockelkorn, D. and Fuchs, G. (2009). Malonic semialdehyde reductase, succinic semialdehyde reductase, and succinyl-coenzyme A reductase from Metallosphaera sedula: enzymes of the autotrophic 3-hydroxypropionate/4-hydroxybutyrate cycle in Sulfolobales. Journal of Bacteriology, 191(20):6352–6362.

Liu, C., Ding, Y., Xian, M., Liu, M., Liu, H., Ma, Q., and Zhao, G. (2017). Malonyl-CoA pathway: a promising route for 3-hydroxypropionate biosynthesis. Critical Reviews in Biotechnology, 37(7):933–941.

Liu, C., Ding, Y., Zhang, R., Liu, H., Xian, M., and Zhao, G. (2016). Functional balance between enzymes in malonyl-CoA pathway for 3-hydroxypropionate biosynthesis. Metabolic Engineering, 34(1):104–111.

Liu, C., Wang, Q., Xian, M., Ding, Y., and Zhao, G. (2013). Dissection of malonyl-coenzyme A reductase of Chloroflexus aurantiacus results in enzyme activity improvement. PloS one, 8(9).

Liu, W., Peterson, P., Langston, J., Jin, X., Zhou, X., Fisher, A., and Toney, M. (2005). Kinetic and crystallographic analysis of active site mutants of Escherichia coli γ-aminobutyrate aminotransferase. Biochemistry, 44(8):2982–2992.

Liu, Z. and Liu, T. (2016). Production of acrylic acid and propionic acid by constructing a portion of the 3-hydroxypropionate/4-hydroxybutyrate cycle from Metallosphaera sedula in Escherichia coli. Journal of Industrial Microbiology and Biotechnology, 43(12):1659–1670.

Machado, D., Rodrigues, L., and Rocha, I. (2014). A kinetic model for curcumin production in Escherichia coli. BioSystems, 125(1):16–21.

Mahadevan, R. and Schilling, C. (2003). The effects of alternate optimal solutions in constraint-based genome-scale metabolic models. *Metabolic engineering*, 5(4):264–276.

Mäntsälä, P. and Zalkin, H. (1976). Properties of apoglutamate synthase and comparison with glutamate dehydrogenase. Journal of Biological Chemistry, 251(11):3300–3305.

Mavrides, C. and Orr, W. (1975). Multispecific aspartate and aromatic amino acid aminotransferases in Escherichia coli. Journal of Biological Chemistry, 250(11):4128–4133.

Meades Jr, G., Benson, B., Grove, A., and Waldrop, G. (2010). A tale of two functions: enzymatic activity and translational repression by carboxyltransferase. Nucleic Acids Research, 38(4):1217–1227.

Millard, P., Smallbone, K., and Mendes, P. (2017). Metabolic regulation is sufficient for global and robust coordination of glucose uptake, catabolism, energy production and growth in Escherichia coli. PLoS Computational Biology, 13(2):1–24.

Monk, J., Lloyd, C., Brunk, E., Mih, N., Sastry, A., King, Z., Takeuchi, R., Nomura, W., Zhang, Z., Mori, H., Feist, A., and Palsson, B. (2017). iML1515, a knowledgebase that computes Escherichia coli traits. Nature Biotechnology, 35(10):904–908.

Pettigrew, D., Yu, G., and Liu, Y. (1990). Nucleotide regulation of Escherichia coli glycerol kinase: Initial-velocity and substrate binding studies. Biochemistry, 29(1):8620–8627.

Piattoni, C., Figueroa, C., Diez, M., Parcerisa, I., Antunã, S., Comelli, R., Guerrero, S., Beccaria, A., and Iglesias, A. (2013). Production and characterization of Escherichia coli glycerol dehydrogenase as a tool for glycerol recycling. Process Biochemistry, 48(3):406–412.

Raj, S., Rathnasingh, C., Jo, J., and Park, S. (2008). Production of 3-hydroxypropionic acid from Glycerol by a novel recombinant Escherichia coli bl21 strain. Process Biochemistry, 43(12):1440–1446.

Raj, S. M., Rathnasingh, C., Jung, W., and Park, S. (2009). Effect of process parameters on 3-hydroxypropionic acid production from Glycerol using a recombinant Escherichia coli. Applied Microbiology and Biotechnology, 84(4):649–657.

Ramjee, M., Genschel, U., Abell, C., and Smith, A. (1997). Escherichia coli L-aspartate-α-decarboxylase: preprotein processing and observation of reaction intermediates by electrospray mass spectrometry. Biochemical Journal, 323(1):661–669.

Rathnasingh, C., Raj, S., Jo, J., and Park, S. (2009). Development and evaluation of efficient recombinant Escherichia coli strains for the production of 3-hydroxypropionic acid from Glycerol. Biotechnology and bioengineering, 104(4):729–739.

Sakamoto, N., Kotre, A., and Savageau, M. (1975). Glutamate dehydrogenase from Escherichia coli: purification and properties. Journal of Bacteriology, 124(2):775–783.

Salles, I., Forchhammer, N., Croux, C., Girbal, L., and Soucaille, P. (2007). Evolution of a Saccharomyces cerevisiae metabolic pathway in Escherichia coli. Metabolic Engineering, 9(2):152–159.

Sauvageot, N., Pichereau, V., Louarme, L., Hartke, A., Auffray, Y., and Laplace, J. (2002). Purification, characterization and subunits identification of the diol dehydratase of Lactobacillus collinoides. European Journal of Biochemistry, 269(22):5731–5737.

Schütz, H. and Radler, F. (1984). Propanediol-1, 2-dehydratase and metabolism of Glycerol of Lactobacillus brevis. Archives of microbiology, 139(4):366–370.

Sharkey, M. and Engel, P. (2008). Apparent negative co-operativity and substrate inhibition in overexpressed glutamate dehydrogenase from Escherichia coli. FEMS Microbiology Letters, 281(2):132–139.

Song, C., Kim, J., Cho, I., and Lee, S. (2016). Metabolic engineering of Escherichia coli for the production of 3-hydroxypropionic acid and malonic acid through β-alanine route. ACS Synthetic Biology, 5(11):1256–1263.

Soriano, A., Radice, A., Herbitter, A., Langsdorf, E., Stafford, J., Chan, S., Wang, S., Liu, Y., and Black, T. (2005). Escherichia coli acetyl-coenzyme a carboxylase: characterization and development of a high-throughput assay. Analytical Biochemistry, 349(2):268–276.

Teufel, R., Kung, J., Kockelkorn, D., Alber, B., and Fuchs, G. (2009). 3-hydroxypropionyl-coenzyme a dehydratase and acryloyl-coenzyme A reductase, enzymes of the autotrophic 3-hydroxypropionate/4-hydroxybutyrate cycle in the Sulfolobales. Journal of Bacteriology, 191(14):4572–4581.

Allied Market Research (2016). Acrylic acid market report. Available at https://www.alliedmarketresearch.com/acrylic-acid-market (2019/10/20).

Thorner, J. and Paulus, H. (1973). Catalytic and allosteric properties of glycerol kinase from Escherichia coli. Journal of Biological Chemistry, 248(11):3922–3932.

Tong, W., Xu, Y., Xian, M., Niu, W., Guo, J., Liu, H., and Zhao, G. (2016). Biosynthetic pathway for acrylic acid from Glycerol in recombinant Escherichia coli. Applied Microbiology and Biotechnology, 100(11):4901–4907.

Unverricht, S., Arnold, H., Tenten, A., Hammon, U., Hans-Peter, N., and Klaus, H. (2006). Method for the catalytic gas phase oxidation of propene into acrylic acid. Patent No.: US6,998,504.

Williamson, J. and Brown, G. (1979). Purification and properties of l-aspartate-alpha-decarboxylase, an enzyme that catalyzes the formation of beta-alanine in Escherichia coli. Journal of Biological Chemistry, 254(16):8074–8082.

Wittig, U., Rey, M., Weidemann, A., Kania, R., and Müller, W. (2018). SABIO-RK: An updated resource for manually curated biochemical reaction kinetics. Nucleic Acids Research, 46(1):656–660.

Yagi, T., Kagamiyama, H., Nozaki, M., and Soda, K. (1985). Glutamate-aspartate transaminase from microorganisms. Methods in Enzymology, 113(1):83–89.

Zhang, H., Lountos, G. T., Ching, C. B., and Jiang, R. (2010). Engineering of glycerol dehydrogenase for improved activity towards 1, 3-butanediol. Applied Microbiology and Biotechnology, 88(1):117–124.

Zhuang, Z., Song, F., Zhao, H., Li, L., Cao, J., Eisenstein, E., Herzberg, O., and Dunaway-Mariano, D. (2008). Divergence of function in the hot dog fold enzyme superfamily: the bacterial thioesterase Ycia. Biochemistry, 47(9):2789–2796.